HAL open science

First observation of a baryonic B_s^0 decay

R. Aaij, B. Adeva, M. Adinolfi, Z. Ajaltouni, S. Akar, J. Albrecht, F. Alessio, M. Alexander, S. Ali, G. Alkhazov, et al.

To cite this version:

R. Aaij, B. Adeva, M. Adinolfi, Z. Ajaltouni, S. Akar, et al.. First observation of a baryonic B_s^0 decay. Physical Review Letters, 2017, 119 (4), pp.041802. 10.1103/PhysRevLett.119.041802 . hal-01582764

HAL Id: hal-01582764

https://hal.science/hal-01582764v1

Submitted on 11 Sep 2023

HAL is a multi-disciplinary open access archive for the deposit and dissemination of scientific research documents, whether they are published or not. The documents may come from teaching and research institutions in France or abroad, or from public or private research centers.

L'archive ouverte pluridisciplinaire **HAL**, est destinée au dépôt et à la diffusion de documents scientifiques de niveau recherche, publiés ou non, émanant des établissements d'enseignement et de recherche français ou étrangers, des laboratoires publics ou privés.

Distributed under a Creative Commons Attribution 4.0 International License

First Observation of a Baryonic B_s^0 Decay

R. Aaij *et al.*[*]
(LHCb Collaboration)

(Received 28 April 2017; published 25 July 2017)

We report the first observation of a baryonic B_s^0 decay, $B_s^0 \to p\bar{\Lambda}K^-$, using proton-proton collision data recorded by the LHCb experiment at center-of-mass energies of 7 and 8 TeV, corresponding to an integrated luminosity of 3.0 fb^{-1}. The branching fraction is measured to be $\mathcal{B}(B_s^0 \to p\bar{\Lambda}K^-) + \mathcal{B}(B_s^0 \to \bar{p}\Lambda K^+) = [5.46 \pm 0.61 \pm 0.57 \pm 0.50(\mathcal{B}) \pm 0.32(f_s/f_d)] \times 10^{-6}$, where the first uncertainty is statistical and the second systematic, the third uncertainty accounts for the experimental uncertainty on the branching fraction of the $B^0 \to p\bar{\Lambda}\pi^-$ decay used for normalization, and the fourth uncertainty relates to the knowledge of the ratio of b-quark hadronization probabilities f_s/f_d.

DOI: 10.1103/PhysRevLett.119.041802

The experimental study of B-meson decays to baryonic final states has a long history, starting with the first observation of baryonic B decays by the CLEO Collaboration in 1997 [1]. The asymmetric e^+e^- collider experiments *BABAR* and Belle reported numerous searches and observations of decays of B^0 and B^+ mesons to baryonic final states [2]. The LHCb Collaboration published the first observation of a baryonic B_c^+ decay in 2014 [3]. Until now, no baryonic B_s^0 decay has ever been observed with a significance in excess of five standard deviations; the Belle Collaboration provided the only evidence for such a process in the study of $B_s^0 \to \bar{\Lambda}_c^- \Lambda \pi^+$ decays, with a significance of 4.4 standard deviations [4].

Areas of particular interest in baryonic B decays are the study of the hierarchy of branching fractions and the threshold enhancement in the baryon-antibaryon mass spectrum [2,5]. Multibody baryonic B decays are expected to have higher branching fractions than two-body decays [6,7]. The $B^0 \to p\bar{\Lambda}\pi^-$ and $B_s^0 \to p\bar{\Lambda}K^-$ branching fractions are predicted to be of the order of 10^{-6} [8]. The notation $B_s^0 \to p\bar{\Lambda}K^-$ is used hereafter for the sum of both accessible final states $B_s^0 \to p\bar{\Lambda}K^-$ and $B_s^0 \to \bar{p}\Lambda K^+$. As emphasized in Ref. [8], which studied the decays $B_s^0 \to p\bar{\Lambda}h^-$, the decay $B_s^0 \to p\bar{\Lambda}K^-$ is a unique baryonic B decay in that it is the only presently known decay where all four processes, namely the decays of a B_s^0 or a $\bar{B}_s^0$ meson to either the $p\bar{\Lambda}K^-$ or the $\bar{p}\Lambda K^+$ final state, can occur. A B -flavor-tagged decay-time-dependent study is required in order to separate the two possible final states and measure their individual branching fractions as well as CP violation observables.

The current experimental knowledge on the family of $B_{(s)}^0 \to p\bar{\Lambda}h^-$ decays ($h = \pi$, K) and related modes such as $B_{(s)}^0 \to p\bar{\Sigma}^0 h^-$, with $\bar{\Sigma}^0 \to \bar{\Lambda}\gamma$, is rather scarce. The $B^0 \to p\bar{\Lambda}\pi^-$ decay has been studied by the *BABAR* [9] and Belle [10,11] collaborations and the Belle Collaboration has reported the 90% confidence level upper limits $\mathcal{B}(B^0 \to p\bar{\Lambda}K^-) < 8.2 \times 10^{-7}$ and $\mathcal{B}(B^0 \to p\bar{\Sigma}^0\pi^-) < 3.8 \times 10^{-6}$ [11].

Manifestations of CP and T violation in baryonic B decays have been studied from a theoretical viewpoint; see for example Ref. [12] and references therein. A large CP-violation asymmetry of order 10% is expected for the $B^0 \to p\bar{\Lambda}\pi^-$ decay mode [12], which further motivates the experimental study of $B_{(s)}^0 \to p\bar{\Lambda}h^-$ decays.

This Letter presents the first observation of a charmless baryonic B_s^0 decay. The branching fraction of the $B_s^0 \to p\bar{\Lambda}K^-$ decay is measured relative to that of the topologically identical $B^0 \to p\bar{\Lambda}\pi^-$ decay to suppress common systematic uncertainties:

$$\mathcal{B}(B_s^0 \to p\bar{\Lambda}K^-) + \mathcal{B}(B_s^0 \to \bar{p}\Lambda K^+) = \frac{f_d}{f_s}\frac{N(B_s^0 \to p\bar{\Lambda}K^-)}{N(B^0 \to p\bar{\Lambda}\pi^-)}\frac{\epsilon_{B^0 \to p\bar{\Lambda}\pi^-}}{\epsilon_{B_s^0 \to p\bar{\Lambda}K^-}}\mathcal{B}(B^0 \to p\bar{\Lambda}\pi^-), \quad (1)$$

where N represents yields determined from mass fits, f_q stands for the b hadronization probability to the meson B_q, and ϵ represents the selection efficiencies. The inclusion of charge-conjugate processes is implied, unless otherwise stated.

The data sample analyzed corresponds to an integrated luminosity of 1.0 fb^{-1} of proton-proton collision data collected by the LHCb experiment at center-of-mass energies of 7 TeV in 2011 and 2.0 fb^{-1} at 8 TeV in 2012. The LHCb detector is a single-arm forward spectrometer covering the pseudorapidity range $2 < \eta < 5$,

[*]Full author list given at the end of the article.

Published by the American Physical Society under the terms of the Creative Commons Attribution 4.0 International license. Further distribution of this work must maintain attribution to the author(s) and the published article's title, journal citation, and DOI.

 © 2017 CERN, for the LHCb Collaboration

designed for the study of particles containing b or c quarks [13,14]. The pseudorapidity is defined as $\eta = -\ln[\tan(\theta/2)]$, where θ is the polar angle with respect to the proton in the positive z direction. The detector elements that are particularly relevant to this analysis are a silicon-strip vertex detector surrounding the proton-proton interaction region that allows heavy hadrons to be identified from their characteristically long flight distance, a tracking system that provides a measurement of momentum, p, of charged particles, two ring-imaging Cherenkov detectors that are able to discriminate between different species of charged hadrons, a calorimeter system for the measurement of photons and neutral hadrons, and multiwire proportional chambers for the detection of muons. Simulated data samples, produced as described in Refs. [15–20], are used to evaluate the response of the detector and to investigate and characterize possible sources of background.

Events are selected in a similar way for both the signal decay $B_s^0 \to p\bar{\Lambda}K^-$ and the normalization channel $B^0 \to p\bar{\Lambda}\pi^-$, where $\bar{\Lambda} \to \bar{p}\pi^+$. Real-time event selection is performed by a trigger [21] consisting of a hardware stage, based on information from the calorimeter and muon systems, followed by a software stage, which performs a full event reconstruction. The hardware trigger stage requires events to have a muon with high transverse momentum, p_T, or a hadron, photon, or electron with high transverse energy deposited in the calorimeters. For this analysis, the hardware trigger decision can either be made on the signal candidates or on other particles in the event. The software trigger requires a two- or three-track secondary vertex with a significant displacement from all the primary pp interaction vertices (PVs). At least one charged particle must have high p_T and be inconsistent with originating from a PV. A multivariate algorithm [22] is used for the identification of secondary vertices consistent with the decay of a b or c hadron.

The Λ decays are reconstructed in two different categories: the first consists of Λ baryons that decay early enough for the proton and pion to be reconstructed in the vertex detector, while the second contains those that decay later such that track segments cannot be reconstructed in the vertex detector. These reconstruction categories are referred to as *long* and *downstream*, respectively.

The selection of $B^0_{(s)}$ candidates, formed by combining a Λ candidate with a proton and a pion or kaon, is carried out with a filtering stage, a requirement on the response of a multilayer perceptron [23] (MLP) classifier, and particle identification (PID) criteria discussed below. The proton and pion or kaon, of opposite charge, both decay products of the B meson, are hereafter referred to as the charged hadrons. Unless stated otherwise, the terms proton and pion refer to the charged hadrons from the B-meson decay, not to the Λ decay products. Both the $B^0 \to p\bar{\Lambda}\pi^-$ and the $B_s^0 \to p\bar{\Lambda}K^-$ decay chains are refitted [24] employing a mass constraint on the Λ candidates.

In the filtering stage the Λ decay products are required to have a minimum momentum, p, form a good quality vertex and satisfy $|m(p\pi^-) - m_\Lambda| < 20(15)\ \mathrm{MeV}/c^2$ for downstream (long) candidates, where m_Λ is the Λ mass [25]. They must have a large impact parameter (IP) with respect to all PVs, where the IP is defined as the minimum distance of a track to a PV. A minimum χ^2_{IP} with respect to any PV is imposed on each Λ decay product, where χ^2_{IP} is defined as the difference between the vertex-fit χ^2 of a PV reconstructed with and without the particle in question. A loose PID requirement, based primarily on information from the ring-imaging Cherenkov detectors, is imposed to select the proton candidate from the Λ baryon to remove background from K_S^0 decays. For downstream Λ candidates a minimum momentum is also required.

A minimum requirement is imposed on the scalar sum of the p_T of the Λ candidate and the two charged hadrons. The distance of closest approach among any pair from (p, $\bar{\Lambda}$, h^-) divided by its uncertainty must be small. The B candidate must have a good quality vertex, have a minimum p_T and a small χ^2_{IP} with respect to the associated PV as its reconstructed momentum vector should point to its production vertex; the associated PV is the one with which it forms the smallest χ^2_{IP}. The pointing condition of the B candidate is further reinforced by requiring that the angle between the B-candidate momentum vector and the line connecting the associated PV and the B-decay vertex (B direction angle, θ_B) is close to zero.

Backgrounds from the $B^0 \to \bar{\Lambda}_c^- p$ decay with $\bar{\Lambda}_c^- \to \bar{\Lambda}\pi^-$ ($\bar{\Lambda}_c^- \to \bar{\Lambda}K^-$) are removed from the $p\bar{\Lambda}\pi^-$ ($p\bar{\Lambda}K^-$) samples with a veto around the Λ_c^+ mass [25] of three times the $\bar{\Lambda}\pi^-$ ($\bar{\Lambda}K^-$) invariant mass resolution of approximately $6\ \mathrm{MeV}/c^2$. No veto is found to be necessary to suppress backgrounds from B decays to charmonia and $\pi^+\pi^-$ pair final states.

Further separation between signal and combinatorial background candidates relies on MLPs implemented with the TMVA toolkit [26]. The MLPs are trained using simulated $B^0 \to p\bar{\Lambda}\pi^-$ samples, generated according to a constant matrix element without intermediate resonances, to represent the signal, and with data from the high-mass sideband region $5400 < m(p\bar{\Lambda}\pi^-) < 5600\,\mathrm{MeV}/c^2$ for the background, to avoid partially reconstructed backgrounds. Separate MLPs are trained and optimized for each year of data taking and for the two Λ reconstruction categories. Each MLP is used to select both $B^0 \to p\bar{\Lambda}\pi^-$ and $B_s^0 \to p\bar{\Lambda}K^-$ candidates.

The 17 variables used in the MLP classifiers are properties of the B candidate, the charged hadrons, and the Λ decay products. The input variables are the following: the χ^2 per degree of freedom of the kinematic fit of the decay chain [24]; the IP for all particles calculated with respect to the associated PV; the distance of closest approach between the two charged hadrons and the sum of their corresponding

$\chi^2_{\rm IP}$; the Λ candidate decay-length significance with respect to the B vertex, i.e., the decay length divided by its uncertainty; the angle between the Λ momentum and the spacial vector connecting the B and Λ decay vertices in the B rest frame; the Λ decay time; the B-meson $p_{\rm T}$, pseudorapidity, direction angle θ_B, decay-length significance and decay time; the Λ helicity angle defined by the Λ momentum in the B rest frame and the boost axis of the B meson, which is given by the B-meson momentum in the laboratory frame; and the pointing variable defined as $P = [\sum_{p,\bar{\Lambda},h^-} p \times \sin\theta_B]/[\sum_{p,\bar{\Lambda},h^-} p \times \sin\theta_B + \sum_{p,\bar{\Lambda},h^-} p_{\rm T}]$. The optimal MLP requirement for each of the four subsamples is determined by maximizing the signal significance of the $B^0 \to p\bar{\Lambda}\pi^-$ normalization decay, with the variation of the signal efficiency with the MLP cut value determined from simulation.

A PID selection is applied to the charged hadrons after the MLP selection. No additional PID requirement is applied to the proton from the Λ candidate since no contamination from misidentified $K^0_S \to \pi^+\pi^-$ decays is observed. The optimization of the PID requirements follows the same procedure as the optimization of the MLP selection. If more than one candidate is selected in any event of any subsample, which occurs in about 5% of selected events, one is chosen at random.

Large data control samples of $D^0 \to K^-\pi^+$, $\Lambda \to p\pi^-$, and $\Lambda_c^+ \to pK^-\pi^+$ decays are employed [27] to determine the efficiency of the PID requirements. All other selection efficiencies are determined from simulation. It is necessary to account for the distribution of signal candidates and the variation of the efficiency over the phase space of the decay. The variation is well described by the factorized efficiencies in the two-dimensional space of the variables $m^2(p\bar{\Lambda})$ and $m^2(ph^-)$ defining the Dalitz plot. Simulated events are binned in $m^2(p\bar{\Lambda})$ in order to determine the selection efficiencies, the variation in $m^2(ph^-)$ being mild and therefore integrated out. The distribution of signal decays in the phase space is obtained separately for each spectrum with the *sPlot* technique [28] with the B-meson candidate invariant mass used as the discriminating variable. The overall efficiencies of this analysis are of order 10^{-4}.

The efficiency of the software trigger selection on both decay modes varied during the data-taking period. During the 2011 data taking, downstream tracks were not reconstructed in the software trigger. Such tracks were included in the trigger during the 2012 data taking and a further significant improvement in the algorithms was implemented mid-year. The corresponding changes to the trigger efficiency are taken into account.

Potential sources of background to the $p\bar{\Lambda}h^-$ spectra are investigated using simulation samples. Cross-feed between the $B^0 \to p\bar{\Lambda}\pi^-$ and $B^0_s \to p\bar{\Lambda}K^-$ decay modes is the dominant source of peaking background. The loop-mediated decays $B^0 \to p\bar{\Lambda}K^-$ and $B^0_s \to p\bar{\Lambda}\pi^-$ are suppressed and estimated to be insignificant [8]. Pion-kaon misidentification from b-baryon decays such as the recently observed decays $\Lambda^0_b \to \Lambda h^+h'^-$ [29] is found to be negligible. The influence of proton-pion misidentification in the reconstruction and selection of the Λ baryon arising from K^0_S cross-feed is checked since the PID requirement on the proton from the Λ is rather loose. It is verified with Armenteros-Podolanski plots [30] that the K^0_S contamination can be ignored. Cross-feed from the presently unobserved decay $\Lambda^0_b \to \Lambda p\bar{p}$ due to proton-pion and proton-kaon misidentification is assumed to be negligible considering that the proton misidentification rate is small. Partially reconstructed decays such as the unobserved $B^0 \to p\bar{\Lambda}\rho^-$ and $B^0_s \to p\bar{\Lambda}K^{*-}$ modes are treated as a source of systematic uncertainty. Decay modes containing a $\bar{\Sigma}^0$ baryon decaying into $\bar{\Sigma}^0 \to \bar{\Lambda}\gamma$, where the γ is not detected, can pollute the signal regions due to the small mass difference $m(\Sigma^0) - m(\Lambda) \approx 77\ {\rm MeV}/c^2$ [25]. The decay $B^0 \to p\bar{\Sigma}^0\pi^-$ is expected to have a branching fraction at the level of 10^{-6} [31], though searches for the $B^0_{(s)} \to p\bar{\Sigma}^0h^-$ family of decays have found no signal [11]. The decays $B^0 \to p\bar{\Sigma}^0\pi^-$ and $B^0_s \to p\bar{\Sigma}^0K^-$ are expected to be the dominant members of the family and are included in the fits to the data.

The yields of the signal and background candidates in eight subsamples are determined from a simultaneous unbinned extended maximum likelihood fit to the $p\bar{\Lambda}h^-$ invariant mass distributions. The eight subsamples correspond to the 2011 and 2012 data-taking periods, the two Λ reconstruction categories, and the $p\bar{\Lambda}\pi^-$ and $p\bar{\Lambda}K^-$ final state hypotheses. This approach allows the use of common shape parameters, and the level of cross-feed background can be better constrained by fitting all subsamples simultaneously. The probability density function in each subsample is defined as the sum of components accounting for the signal decay, the cross-feed contribution, the $B^0 \to p\bar{\Sigma}^0\pi^-$ and $B^0_s \to p\bar{\Sigma}^0K^-$ decays, and combinatorial background.

The signal and normalization modes are modeled with the sum of two Novosibirsk functions [32]. All shape parameters are fixed to the values obtained separately for each subsample from simulation samples. The $B^0 \to p\bar{\Lambda}\pi^-$ and $B^0_s \to p\bar{\Lambda}K^-$ peak positions are free parameters determined simultaneously in all subsamples. The cross-feed $B^0_s \to p\bar{\Lambda}K^-$ ($B^0 \to p\bar{\Lambda}\pi^-$) in the $p\bar{\Lambda}\pi^-$ ($p\bar{\Lambda}K^-$) invariant mass distribution is modeled with the sum of a Gaussian and a modified Fermi function defined as the product of an exponential and a Fermi-Dirac function. The $B^0 \to p\bar{\Sigma}^0\pi^-$ and $B^0_s \to p\bar{\Sigma}^0K^-$ decays are modeled differently according to the Λ reconstruction category and the $p\bar{\Lambda}h^-$ invariant mass hypothesis under which they are reconstructed. Depending on the category, a modified Fermi function, a sum of two Novosibirsk functions, the sum of a Novosibirsk and a Gaussian function, or the sum of a Novosibirsk and a modified Fermi function, are used.

A combinatorial background component described by an exponential function is present for both $p\bar{\Lambda}h^-$ final states.

The yields of the $B^0 \to p\bar{\Lambda}\pi^-$ candidates are determined in the fit together with the ratio of the $B_s^0 \to p\bar{\Lambda}K^-$ to $B^0 \to p\bar{\Lambda}\pi^-$ branching fractions, which is determined simultaneously across all subsamples accounting for differences in selection efficiencies. These depend on the data-taking period, Λ reconstruction category, and mass hypothesis of the meson from the B decay. The uncertainties arising from the ratios of efficiencies are included in the fit as Gaussian constraints. The yields of the $B^0 \to p\bar{\Sigma}^0\pi^-$ and $B_s^0 \to p\bar{\Sigma}^0K^-$ decays are defined relative to those of the corresponding $B^0 \to p\bar{\Lambda}\pi^-$ and $B_s^0 \to p\bar{\Lambda}K^-$ decays, respectively. These two Σ^0-to-Λ decay yield ratios are determined simultaneously in the fit across all subsamples following the same procedure as for the $B_s^0 \to p\bar{\Lambda}K^-$ decay. The combinatorial background yield and shape parameters are treated independently in each subsample and are allowed to vary in the fit.

Figure 1 presents the fit to the $p\bar{\Lambda}h^-$ invariant mass distributions for all subsamples combined. Both $B^0 \to p\bar{\Lambda}\pi^-$ and $B_s^0 \to p\bar{\Lambda}K^-$ signals are prominent. In particular, the $B_s^0 \to p\bar{\Lambda}K^-$ decay is observed with a statistical significance above 15 standard deviations, estimated from the change in log-likelihood between fits with and without the $B_s^0 \to p\bar{\Lambda}K^-$ signal component [33]. It constitutes the first observation of a baryonic B_s^0 decay. The yields summed over all subsamples are $N(B^0 \to p\bar{\Lambda}\pi^-) = 519 \pm 28$ and $N(B_s^0 \to p\bar{\Lambda}K^-) = 234 \pm 29$, where the uncertainties are statistical only.

The *sPlot* technique is used to subtract the background and obtain the phase space distribution of signal candidates. Figure 2 shows the $m(p\bar{\Lambda})$ invariant mass distributions for the $B^0 \to p\bar{\Lambda}\pi^-$ and $B_s^0 \to p\bar{\Lambda}K^-$ candidates after correcting for the distribution selection efficiencies. Both distributions show a pronounced enhancement at threshold

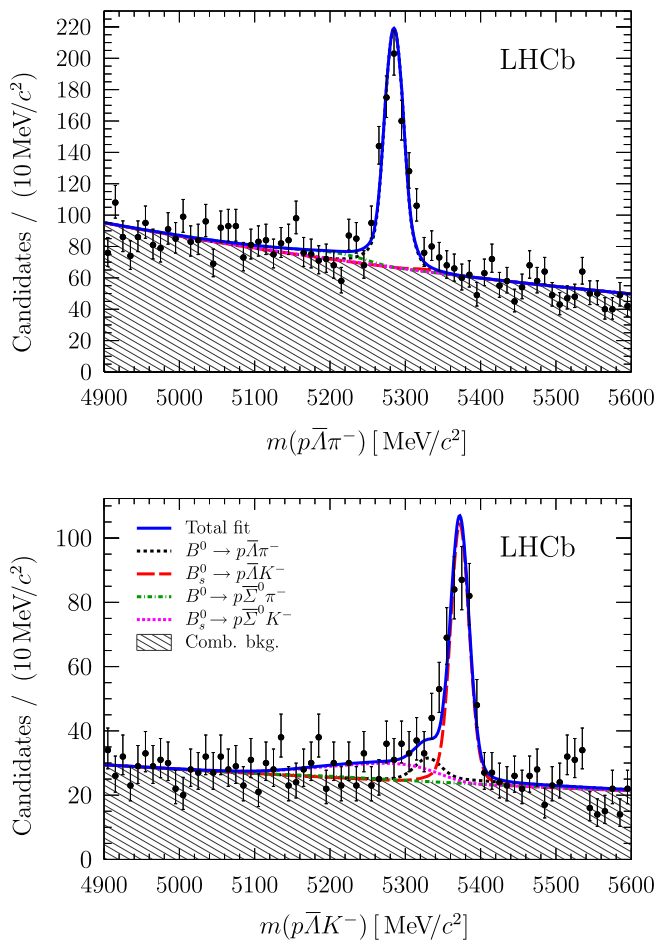

FIG. 1. Mass distributions for b-hadron candidates for (top) the $p\bar{\Lambda}\pi^-$ and (bottom) the $p\bar{\Lambda}K^-$ sample for the combined long and downstream categories. The black points represent the data, the solid blue curve the result of the fit, the red dashed curve the $B_s^0 \to p\bar{\Lambda}K^-$ contribution, the black (magenta) dotted curve the $B^0 \to p\bar{\Lambda}\pi^-$ ($B_s^0 \to p\bar{\Sigma}^0K^-$) and the green dash-dotted curve the contribution from $B^0 \to p\bar{\Sigma}^0\pi^-$ decays. The combinatorial background distribution is indicated by the shaded histogram.

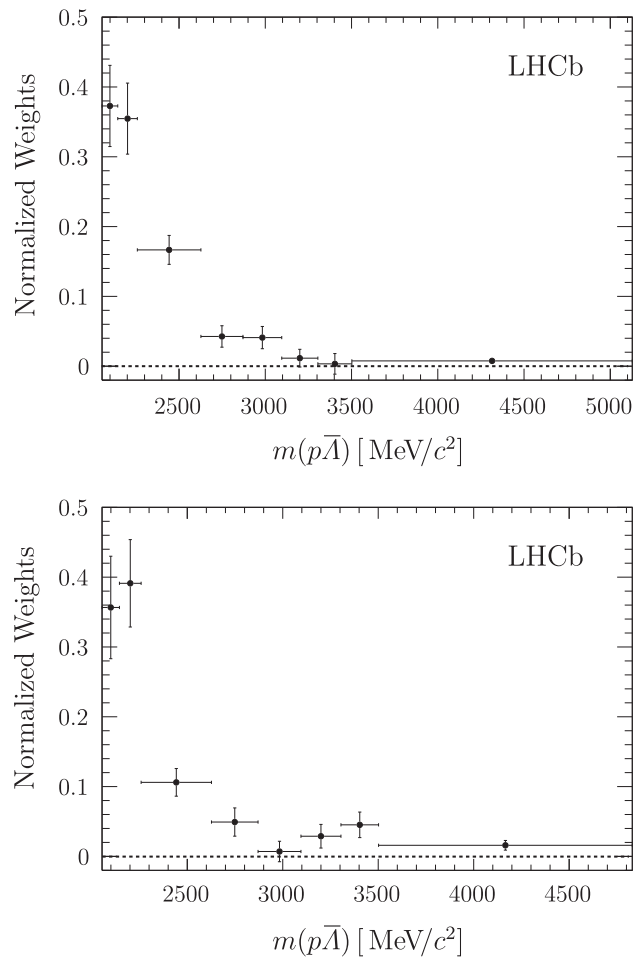

FIG. 2. Efficiency-corrected and background-subtracted $m(p\bar{\Lambda})$ invariant mass distributions for (top) $B^0 \to p\bar{\Lambda}\pi^-$ and (bottom) $B_s^0 \to p\bar{\Lambda}K^-$ candidates. The distributions are normalized to unity.

in the baryon-antibaryon invariant mass, first suggested in Ref. [5] and observed in several baryonic B decay modes.

The sources of systematic uncertainty arise from the fit model, the knowledge of the selection efficiencies, and the uncertainties on the $B^0 \to p\bar{\Lambda}\pi^-$ branching fraction and on the ratio of hadronization probabilities f_s/f_d. Uncertainties on the selection efficiencies arise from residual differences between data and simulation in the trigger, reconstruction, selection, and particle identification. Additional uncertainties arise due to the limited size of the simulation samples and the corresponding uncertainty on the distribution of the efficiencies across the decay phase space. As the efficiencies depend on the signal decay-time distribution, the effect coming from the different lifetimes of the B_s^0 mass eigenstates has been evaluated [34]. Pseudoexperiments are used to estimate the effect of using alternative shapes for the fit components, of including additional backgrounds in the fit such as partially reconstructed decays, and of excluding the $B^0 \to p\bar{\Sigma}^0\pi^-$ and $B_s^0 \to p\bar{\Sigma}^0 K^-$ decays that show no significant contribution. Intrinsic biases in the fitted signal yields are investigated with ensembles of simulated pseudoexperiments. A small bias is found and added to the systematic uncertainty on the fit model. The systematic uncertainty due to the knowledge of the efficiencies involved in the definition of fit constraints is negligible. The total systematic uncertainty on the $B_s^0 \to p\bar{\Lambda}K^-$ branching fraction is given by the sum of all uncertainties added in quadrature and amounts to 10.5%; it is dominated by the systematic uncertainty on the fit model.

The uncertainty on the branching fraction of the normalization decay, $\mathcal{B}(B^0 \to p\bar{\Lambda}\pi^-) = (3.14 \pm 0.29) \times 10^{-6}$ [25], is taken as a systematic uncertainty from external inputs. The 5.8% uncertainty on the latest f_s/f_d combination from LHCb, $f_s/f_d = 0.259 \pm 0.015$ [35], is taken as a second source of systematic uncertainty from external inputs.

The $B_s^0 \to p\bar{\Lambda}K^-$ branching fraction, determined relative to that of the $B^0 \to p\bar{\Lambda}\pi^-$ normalization channel according to Eq. (1), is measured to be

$$\mathcal{B}(B_s^0 \to p\bar{\Lambda}K^-) + \mathcal{B}(B_s^0 \to \bar{p}\Lambda K^+) = [5.46 \pm 0.61 \pm 0.57 \pm 0.50(\mathcal{B}) \pm 0.32(f_s/f_d)] \times 10^{-6},$$

where the first uncertainty is statistical and the second systematic, the third uncertainty accounts for the experimental uncertainty on the branching fraction of the $B^0 \to p\bar{\Lambda}\pi^-$ decay, and the fourth uncertainty relates to the knowledge of f_s/f_d.

In summary, the first observation of the three-body charmless baryonic decay $B_s^0 \to p\bar{\Lambda}K^-$ is reported using a proton-proton collision data sample collected by the LHCb experiment, corresponding to an integrated luminosity of 3.0 fb^{-1}. The decay is observed with a statistical significance above 15 standard deviations, which constitutes the first observation of a baryonic B_s^0 decay.

Decays of B mesons to final states containing baryons are now observed for all B-meson species. Their study provides valuable information on the dynamics of hadronic decays of B mesons. The present analysis motivates further theoretical studies of baryonic B_s^0 decays in addition to those currently published [6,8,36,37].

We express our gratitude to our colleagues in the CERN accelerator departments for the excellent performance of the LHC. We thank the technical and administrative staff at the LHCb institutes. We acknowledge support from CERN and from the national agencies: CAPES, CNPq, FAPERJ and FINEP (Brazil); MOST and NSFC (People's Republic of China); CNRS/IN2P3 (France); BMBF, DFG and MPG (Germany); INFN (Italy); NWO (The Netherlands); MNiSW and NCN (Poland); MEN/IFA (Romania); MinES and FASO (Russia); MinECo (Spain); SNSF and SER (Switzerland); NASU (Ukraine); STFC (United Kingdom); NSF (USA). We acknowledge the computing resources that are provided by CERN, IN2P3 (France), KIT and DESY (Germany), INFN (Italy), SURF (The Netherlands), PIC (Spain), GridPP (United Kingdom), RRCKI and Yandex LLC (Russia), CSCS (Switzerland), IFIN-HH (Romania), CBPF (Brazil), PL-GRID (Poland) and OSC (USA). We are indebted to the communities behind the multiple open source software packages on which we depend. Individual groups or members have received support from AvH Foundation (Germany), EPLANET, Marie Skłodowska-Curie Actions and ERC (European Union), Conseil Général de Haute-Savoie, Labex ENIGMASS and OCEVU, Région Auvergne (France), RFBR and Yandex LLC (Russia), GVA, XuntaGal and GENCAT (Spain), Herchel Smith Fund, The Royal Society, Royal Commission for the Exhibition of 1851 and the Leverhulme Trust (United Kingdom).

[1] X. Fu *et al.* (CLEO Collaboration), Observation of Exclusive B Decays to Final States Containing a Charmed Baryon, Phys. Rev. Lett. **79**, 3125 (1997).
[2] A. J. Bevan *et al.* (*BABAR* and Belle Collaborations), The physics of the B factories, Eur. Phys. J. C **74**, 3026 (2014).
[3] R. Aaij *et al.* (LHCb Collaboration), First Observation of a Baryonic B_c^+ decay, Phys. Rev. Lett. **113**, 152003 (2014).
[4] E. Solovieva *et al.* (Belle Collaboration), Evidence for $\bar{B}_s^0 \to \Lambda_c^+\bar{\Lambda}\pi^-$, Phys. Lett. B **726**, 206 (2013).
[5] W.-S. Hou and A. Soni, Pathways to Rare Baryonic B Decays, Phys. Rev. Lett. **86**, 4247 (2001).
[6] Y. K. Hsiao and C. Q. Geng, Violation of partial conservation of the axial-vector current and two-body baryonic B and D_s decays, Phys. Rev. D **91**, 077501 (2015).
[7] H.-Y. Cheng and C.-K. Chua, On the smallness of tree-dominated charmless two-body baryonic B decay rates, Phys. Rev. D **91**, 036003 (2015).

[8] C. Q. Geng, Y. K. Hsiao, and E. Rodrigues, Three-body charmless baryonic $\bar{B}_s^0$ decays, Phys. Lett. B **767**, 205 (2017).
[9] B. Aubert *et al.* (*BABAR* Collaboration), Measurement of the branching fraction and $\bar{\Lambda}$ polarization in $B^0 \to \bar{\Lambda} p \pi^-$, Phys. Rev. D **79**, 112009 (2009).
[10] M.-Z. Wang *et al.* (Belle Collaboration), Study of $B^+ \to p\bar{\Lambda}\gamma$, $p\bar{\Lambda}\pi^0$ and $B^0 \to p\bar{\Lambda}\pi^-$, Phys. Rev. D **76**, 052004 (2007).
[11] M. Z. Wang *et al.* (Belle Collaboration), Observation of $B^0 \to p\bar{\Lambda}\pi^-$, Phys. Rev. Lett. **90**, 201802 (2003).
[12] C. Q. Geng and Y. K. Hsiao, Direct CP and T violation in baryonic B decays, Int. J. Mod. Phys. A **23**, 3290 (2008).
[13] A. A. Alves Jr. *et al.* (LHCb Collaboration), The LHCb detector at the LHC, J. Instrum. **3**, S08005 (2008).
[14] R. Aaij *et al.* (LHCb Collaboration), LHCb detector performance, Int. J. Mod. Phys. A **30**, 1530022 (2015).
[15] T. Sjöstrand, S. Mrenna, and P. Skands, A brief introduction to PYTHIA 8.1, Comput. Phys. Commun. **178**, 852 (2008); T. Sjöstrand, S. Mrenna, and P. Skands, PYTHIA 6.4 physics and manual, J. High Energy Phys. 05 (2006) 026.
[16] I. Belyaev *et al.*, Handling of the generation of primary events in Gauss, the LHCb simulation framework, J. Phys. Conf. Ser. **331**, 032047 (2011).
[17] D. J. Lange, The EvtGen particle decay simulation package, Nucl. Instrum. Methods Phys. Res., Sect. A **462**, 152 (2001).
[18] P. Golonka and Z. Was, PHOTOS Monte Carlo: A precision tool for QED corrections in Z and W decays, Eur. Phys. J. C **45**, 97 (2006).
[19] J. Allison *et al.* (Geant4 Collaboration), Geant4 developments and applications, IEEE Trans. Nucl. Sci. **53**, 270 (2006); S. Agostinelli *et al.* (Geant4 Collaboration), Geant4: A simulation toolkit, Nucl. Instrum. Methods Phys. Res., Sect. A **506**, 250 (2003).
[20] M. Clemencic, G. Corti, S. Easo, C. R. Jones, S. Miglioranzi, M. Pappagallo, and P. Robbe, The LHCb simulation application, Gauss: Design, evolution and experience, J. Phys. Conf. Ser. **331**, 032023 (2011).
[21] R. Aaij *et al.*, The LHCb trigger and its performance in 2011, J. Instrum. **8**, P04022 (2013).
[22] V. V. Gligorov and M. Williams, Efficient, reliable and fast high-level triggering using a bonsai boosted decision tree, J. Instrum. **8**, P02013 (2013).
[23] D. E. Rumelhart, G. E. Hinton, and R. J. Williams, *Parallel Distributed Processing: Explorations in the Microstructure of Cognition* (MIT, Cambridge, USA, 1986), Vol. 1.
[24] W. D. Hulsbergen, Decay chain fitting with a Kalman filter, Nucl. Instrum. Methods Phys. Res., Sect. A **552**, 566 (2005).
[25] C. Patrignani *et al.* (Particle Data Group), Review of particle physics, Chin. Phys. C **40**, 100001 (2016).
[26] P. Speckmayer, A. Hoecker, J. Stelzer, and H. Voss, The toolkit for multivariate data analysis: TMVA 4, J. Phys. Conf. Ser. **219**, 032057 (2010).
[27] M. Adinolfi *et al.*, Performance of the LHCb RICH detector at the LHC, Eur. Phys. J. C **73**, 2431 (2013).
[28] M. Pivk and F. R. Le Diberder, sPlot: A statistical tool to unfold data distributions, Nucl. Instrum. Methods Phys. Res., Sect. A **555**, 356 (2005).
[29] R. Aaij *et al.* (LHCb Collaboration), Observations of $\Lambda_b^0 \to \Lambda K^+\pi^-$ and $\Lambda_b^0 \to \Lambda K^+K^-$ decays and searches for other Λ_b^0 and Ξ_b^0 decays to Λh^+h^- final states, J. High Energy Phys. 05 (2016) 081.
[30] J. Podolanski and R. Armenteros, III. Analysis of V-events, The London, Edinburgh, and Dublin Philosophical Magazine and Journal of Science **45**, 13 (1954).
[31] C.-K. Chua, W.-S. Hou, and S.-Y. Tsai, Charmless three-body baryonic B decays, Phys. Rev. D **66**, 054004 (2002).
[32] B. Aubert *et al.* (*BABAR* Collaboration), in *Proceedings of the 31st International Conference on High Energy Physics, ICHEP 2002, Amsterdam, Netherlands, 2002*, arXiv:hep-ex/0207083.
[33] S. S. Wilks, The large-sample distribution of the likelihood ratio for testing composite hypotheses, Ann. Math. Stat. **9**, 60 (1938).
[34] K. De Bruyn, R. Fleischer, R. Knegjens, P. Koppenburg, M. Merk, and N. Tuning, Branching ratio measurements of B_s^0 decays, Phys. Rev. D **86**, 014027 (2012).
[35] R. Aaij *et al.* (LHCb Collaboration), Measurement of the fragmentation fraction ratio f_s/f_d and its dependence on B meson kinematics, J. High Energy Phys. 04 (2013) 001; f_s/f_d value updated in LHCb-CONF-2013-011.
[36] Y. K. Hsiao and C. Q. Geng, $f_J(2220)$ and hadronic $\bar{B}_s^0$ decays, Eur. Phys. J. C **75**, 101 (2015).
[37] C.-K. Chua, Charmless two-body baryonic $B_{u,d,s}$ decays revisited, Phys. Rev. D **89**, 056003 (2014).

R. Aaij,[40] B. Adeva,[39] M. Adinolfi,[48] Z. Ajaltouni,[5] S. Akar,[59] J. Albrecht,[10] F. Alessio,[40] M. Alexander,[53] S. Ali,[43] G. Alkhazov,[31] P. Alvarez Cartelle,[55] A. A. Alves Jr.,[59] S. Amato,[2] S. Amerio,[23] Y. Amhis,[7] L. An,[3] L. Anderlini,[18] G. Andreassi,[41] M. Andreotti,[17,a] J. E. Andrews,[60] R. B. Appleby,[56] F. Archilli,[43] P. d'Argent,[12] J. Arnau Romeu,[6] A. Artamonov,[37] M. Artuso,[61] E. Aslanides,[6] G. Auriemma,[26] M. Baalouch,[5] I. Babuschkin,[56] S. Bachmann,[12] J. J. Back,[50] A. Badalov,[38] C. Baesso,[62] S. Baker,[55] V. Balagura,[7,b] W. Baldini,[17] A. Baranov,[35] R. J. Barlow,[56] C. Barschel,[40] S. Barsuk,[7] W. Barter,[56] F. Baryshnikov,[32] M. Baszczyk,[27,c] V. Batozskaya,[29] V. Battista,[41] A. Bay,[41] L. Beaucourt,[4] J. Beddow,[53] F. Bedeschi,[24] I. Bediaga,[1] A. Beiter,[61] L. J. Bel,[43] V. Bellee,[41] N. Belloli,[21,d] K. Belous,[37] I. Belyaev,[32] E. Ben-Haim,[8] G. Bencivenni,[19] S. Benson,[43] S. Beranek,[9] A. Berezhnoy,[33] R. Bernet,[42] A. Bertolin,[23] C. Betancourt,[42] F. Betti,[15] M.-O. Bettler,[40] M. van Beuzekom,[43] Ia. Bezshyiko,[42] S. Bifani,[47] P. Billoir,[8] A. Birnkraut,[10] A. Bitadze,[56] A. Bizzeti,[18,e] T. Blake,[50] F. Blanc,[41] J. Blouw,[11] S. Blusk,[61] V. Bocci,[26] T. Boettcher,[58] A. Bondar,[36,f] N. Bondar,[31] W. Bonivento,[16]

I. Bordyuzhin,[32] A. Borgheresi,[21,d] S. Borghi,[56] M. Borisyak,[35] M. Borsato,[39] F. Bossu,[7] M. Boubdir,[9] T. J. V. Bowcock,[54] E. Bowen,[42] C. Bozzi,[17,40] S. Braun,[12] T. Britton,[61] J. Brodzicka,[56] E. Buchanan,[48] C. Burr,[56] A. Bursche,[16] J. Buytaert,[40] S. Cadeddu,[16] R. Calabrese,[17,a] M. Calvi,[21,d] M. Calvo Gomez,[38,g] A. Camboni,[38] P. Campana,[19] D. H. Campora Perez,[40] L. Capriotti,[56] A. Carbone,[15,h] G. Carboni,[25,i] R. Cardinale,[20,j] A. Cardini,[16] P. Carniti,[21,d] L. Carson,[52] K. Carvalho Akiba,[2] G. Casse,[54] L. Cassina,[21,d] L. Castillo Garcia,[41] M. Cattaneo,[40] G. Cavallero,[20,40,j] R. Cenci,[24,k] D. Chamont,[7] M. Charles,[8] Ph. Charpentier,[40] G. Chatzikonstantinidis,[47] M. Chefdeville,[4] S. Chen,[56] S. F. Cheung,[57] V. Chobanova,[39] M. Chrzaszcz,[42,27] A. Chubykin,[31] X. Cid Vidal,[39] G. Ciezarek,[43] P. E. L. Clarke,[52] M. Clemencic,[40] H. V. Cliff,[49] J. Closier,[40] V. Coco,[59] J. Cogan,[6] E. Cogneras,[5] V. Cogoni,[16,l] L. Cojocariu,[30] P. Collins,[40] A. Comerma-Montells,[12] A. Contu,[40] A. Cook,[48] G. Coombs,[40] S. Coquereau,[38] G. Corti,[40] M. Corvo,[17,a] C. M. Costa Sobral,[50] B. Couturier,[40] G. A. Cowan,[52] D. C. Craik,[52] A. Crocombe,[50] M. Cruz Torres,[62] S. Cunliffe,[55] R. Currie,[52] C. D'Ambrosio,[40] F. Da Cunha Marinho,[2] E. Dall'Occo,[43] J. Dalseno,[48] A. Davis,[3] O. De Aguiar Francisco,[54] K. De Bruyn,[6] S. De Capua,[56] M. De Cian,[12] J. M. De Miranda,[1] L. De Paula,[2] M. De Serio,[14,m] P. De Simone,[19] C. T. Dean,[53] D. Decamp,[4] M. Deckenhoff,[10] L. Del Buono,[8] H.-P. Dembinski,[11] M. Demmer,[10] A. Dendek,[28] D. Derkach,[35] O. Deschamps,[5] F. Dettori,[54] B. Dey,[22] A. Di Canto,[40] P. Di Nezza,[19] H. Dijkstra,[40] F. Dordei,[40] M. Dorigo,[41] A. Dosil Suárez,[39] A. Dovbnya,[45] K. Dreimanis,[54] L. Dufour,[43] G. Dujany,[56] K. Dungs,[40] P. Durante,[40] R. Dzhelyadin,[37] M. Dziewiecki,[12] A. Dziurda,[40] A. Dzyuba,[31] N. Déléage,[4] S. Easo,[51] M. Ebert,[52] U. Egede,[55] V. Egorychev,[32] S. Eidelman,[36,f] S. Eisenhardt,[52] U. Eitschberger,[10] R. Ekelhof,[10] L. Eklund,[53] S. Ely,[61] S. Esen,[12] H. M. Evans,[49] T. Evans,[57] A. Falabella,[15] N. Farley,[47] S. Farry,[54] R. Fay,[54] D. Fazzini,[21,d] D. Ferguson,[52] G. Fernandez,[38] A. Fernandez Prieto,[39] F. Ferrari,[15] F. Ferreira Rodrigues,[2] M. Ferro-Luzzi,[40] S. Filippov,[34] R. A. Fini,[14] M. Fiore,[17,a] M. Fiorini,[17,a] M. Firlej,[28] C. Fitzpatrick,[41] T. Fiutowski,[28] F. Fleuret,[7,n] K. Fohl,[40] M. Fontana,[16,40] F. Fontanelli,[20,j] D. C. Forshaw,[61] R. Forty,[40] V. Franco Lima,[54] M. Frank,[40] C. Frei,[40] J. Fu,[22,o] W. Funk,[40] E. Furfaro,[25,i] C. Färber,[40] E. Gabriel,[52] A. Gallas Torreira,[39] D. Galli,[15,h] S. Gallorini,[23] S. Gambetta,[52] M. Gandelman,[2] P. Gandini,[57] Y. Gao,[3] L. M. Garcia Martin,[70] J. García Pardiñas,[39] J. Garra Tico,[49] L. Garrido,[38] P. J. Garsed,[49] D. Gascon,[38] C. Gaspar,[40] L. Gavardi,[10] G. Gazzoni,[5] D. Gerick,[12] E. Gersabeck,[12] M. Gersabeck,[56] T. Gershon,[50] Ph. Ghez,[4] S. Gianì,[41] V. Gibson,[49] O. G. Girard,[41] L. Giubega,[30] K. Gizdov,[52] V. V. Gligorov,[8] D. Golubkov,[32] A. Golutvin,[55,40] A. Gomes,[1,p] I. V. Gorelov,[33] C. Gotti,[21,d] E. Govorkova,[43] R. Graciani Diaz,[38] L. A. Granado Cardoso,[40] E. Graugés,[38] E. Graverini,[42] G. Graziani,[18] A. Grecu,[30] R. Greim,[9] P. Griffith,[16] L. Grillo,[21,40,d] L. Gruber,[40] B. R. Gruberg Cazon,[57] O. Grünberg,[67] E. Gushchin,[34] Yu. Guz,[37] T. Gys,[40] C. Göbel,[62] T. Hadavizadeh,[57] C. Hadjivasiliou,[5] G. Haefeli,[41] C. Haen,[40] S. C. Haines,[49] B. Hamilton,[60] X. Han,[12] S. Hansmann-Menzemer,[12] N. Harnew,[57] S. T. Harnew,[48] J. Harrison,[56] M. Hatch,[40] J. He,[63] T. Head,[41] A. Heister,[9] K. Hennessy,[54] P. Henrard,[5] L. Henry,[70] E. van Herwijnen,[40] M. Heß,[67] A. Hicheur,[2] D. Hill,[57] C. Hombach,[56] P. H. Hopchev,[41] Z.-C. Huard,[59] W. Hulsbergen,[43] T. Humair,[55] M. Hushchyn,[35] D. Hutchcroft,[54] M. Idzik,[28] P. Ilten,[58] R. Jacobsson,[40] J. Jalocha,[57] E. Jans,[43] A. Jawahery,[60] F. Jiang,[3] M. John,[57] D. Johnson,[40] C. R. Jones,[49] C. Joram,[40] B. Jost,[40] N. Jurik,[57] S. Kandybei,[45] M. Karacson,[40] J. M. Kariuki,[48] S. Karodia,[53] M. Kecke,[12] M. Kelsey,[61] M. Kenzie,[49] T. Ketel,[44] E. Khairullin,[35] B. Khanji,[12] C. Khurewathanakul,[41] T. Kirn,[9] S. Klaver,[56] K. Klimaszewski,[29] T. Klimkovich,[11] S. Koliiev,[46] M. Kolpin,[12] I. Komarov,[41] R. Kopecna,[12] P. Koppenburg,[43] A. Kosmyntseva,[32] S. Kotriakhova,[31] M. Kozeiha,[5] L. Kravchuk,[34] M. Kreps,[50] P. Krokovny,[36,f] F. Kruse,[10] W. Krzemien,[29] W. Kucewicz,[27,c] M. Kucharczyk,[27] V. Kudryavtsev,[36,f] A. K. Kuonen,[41] K. Kurek,[29] T. Kvaratskheliya,[32,40] D. Lacarrere,[40] G. Lafferty,[56] A. Lai,[16] G. Lanfranchi,[19] C. Langenbruch,[9] T. Latham,[50] C. Lazzeroni,[47] R. Le Gac,[6] J. van Leerdam,[43] A. Leflat,[33,40] J. Lefrançois,[7] R. Lefèvre,[5] F. Lemaitre,[40] E. Lemos Cid,[39] O. Leroy,[6] T. Lesiak,[27] B. Leverington,[12] T. Li,[3] Y. Li,[7] Z. Li,[61] T. Likhomanenko,[35,68] R. Lindner,[40] F. Lionetto,[42] X. Liu,[3] D. Loh,[50] I. Longstaff,[53] J. H. Lopes,[2] D. Lucchesi,[23,q] M. Lucio Martinez,[39] H. Luo,[52] A. Lupato,[23] E. Luppi,[17,a] O. Lupton,[40] A. Lusiani,[24] X. Lyu,[63] F. Machefert,[7] F. Maciuc,[30] B. Maddock,[59] O. Maev,[31] K. Maguire,[56] S. Malde,[57] A. Malinin,[68] T. Maltsev,[36] G. Manca,[16,l] G. Mancinelli,[6] P. Manning,[61] J. Maratas,[5,r] J. F. Marchand,[4] U. Marconi,[15] C. Marin Benito,[38] M. Marinangeli,[41] P. Marino,[24,k] J. Marks,[12] G. Martellotti,[26] M. Martin,[6] M. Martinelli,[41] D. Martinez Santos,[39] F. Martinez Vidal,[70] D. Martins Tostes,[2] L. M. Massacrier,[7] A. Massafferri,[1] R. Matev,[40] A. Mathad,[50] Z. Mathe,[40] C. Matteuzzi,[21] A. Mauri,[42] E. Maurice,[7,n] B. Maurin,[41] A. Mazurov,[47] M. McCann,[55,40] A. McNab,[56] R. McNulty,[13] B. Meadows,[59] F. Meier,[10] D. Melnychuk,[29] M. Merk,[43] A. Merli,[22,40,o] E. Michielin,[23] D. A. Milanes,[66] M.-N. Minard,[4] D. S. Mitzel,[12] A. Mogini,[8] J. Molina Rodriguez,[1] I. A. Monroy,[66] S. Monteil,[5] M. Morandin,[23] M. J. Morello,[24,k] O. Morgunova,[68] J. Moron,[28] A. B. Morris,[52] R. Mountain,[61] F. Muheim,[52] M. Mulder,[43] M. Mussini,[15] D. Müller,[56] J. Müller,[10] K. Müller,[42] V. Müller,[10]

P. Naik,[48] T. Nakada,[41] R. Nandakumar,[51] A. Nandi,[57] I. Nasteva,[2] M. Needham,[52] N. Neri,[22,40] S. Neubert,[12] N. Neufeld,[40] M. Neuner,[12] T. D. Nguyen,[41] C. Nguyen-Mau,[41,s] S. Nieswand,[9] R. Niet,[10] N. Nikitin,[33] T. Nikodem,[12] A. Nogay,[68] D. P. O'Hanlon,[50] A. Oblakowska-Mucha,[28] V. Obraztsov,[37] S. Ogilvy,[19] R. Oldeman,[16,l] C. J. G. Onderwater,[71] A. Ossowska,[27] J. M. Otalora Goicochea,[2] P. Owen,[42] A. Oyanguren,[70] P. R. Pais,[41] A. Palano,[14,m] M. Palutan,[19,40] A. Papanestis,[51] M. Pappagallo,[14,m] L. L. Pappalardo,[17,a] C. Pappenheimer,[59] W. Parker,[60] C. Parkes,[56] G. Passaleva,[18] A. Pastore,[14,m] M. Patel,[55] C. Patrignani,[15,h] A. Pearce,[40] A. Pellegrino,[43] G. Penso,[26] M. Pepe Altarelli,[40] S. Perazzini,[40] P. Perret,[5] L. Pescatore,[41] K. Petridis,[48] A. Petrolini,[20,j] A. Petrov,[68] M. Petruzzo,[22,o] E. Picatoste Olloqui,[38] B. Pietrzyk,[4] M. Pikies,[27] D. Pinci,[26] A. Pistone,[20,j] A. Piucci,[12] V. Placinta,[30] S. Playfer,[52] M. Plo Casasus,[39] T. Poikela,[40] F. Polci,[8] M. Poli Lener,[19] A. Poluektov,[50,36] I. Polyakov,[61] E. Polycarpo,[2] G. J. Pomery,[48] S. Ponce,[40] A. Popov,[37] D. Popov,[11,40] B. Popovici,[30] S. Poslavskii,[37] C. Potterat,[2] E. Price,[48] J. Prisciandaro,[39] C. Prouve,[48] V. Pugatch,[46] A. Puig Navarro,[42] G. Punzi,[24,t] C. Qian,[63] W. Qian,[50] R. Quagliani,[7,48] B. Rachwal,[28] J. H. Rademacker,[48] M. Rama,[24] M. Ramos Pernas,[39] M. S. Rangel,[2] I. Raniuk,[45] F. Ratnikov,[35] G. Raven,[44] M. Ravonel Salzgeber,[40] M. Reboud,[4] F. Redi,[55] S. Reichert,[10] A. C. dos Reis,[1] C. Remon Alepuz,[70] V. Renaudin,[7] S. Ricciardi,[51] S. Richards,[48] M. Rihl,[40] K. Rinnert,[54] V. Rives Molina,[38] P. Robbe,[7] A. B. Rodrigues,[1] E. Rodrigues,[59] J. A. Rodriguez Lopez,[66] P. Rodriguez Perez,[56] A. Rogozhnikov,[35] S. Roiser,[40] A. Rollings,[57] V. Romanovskiy,[37] A. Romero Vidal,[39] J. W. Ronayne,[13] M. Rotondo,[19] M. S. Rudolph,[61] T. Ruf,[40] P. Ruiz Valls,[70] J. J. Saborido Silva,[39] E. Sadykhov,[32] N. Sagidova,[31] B. Saitta,[16,l] V. Salustino Guimaraes,[1] D. Sanchez Gonzalo,[38] C. Sanchez Mayordomo,[70] B. Sanmartin Sedes,[39] R. Santacesaria,[26] C. Santamarina Rios,[39] M. Santimaria,[19] E. Santovetti,[25,i] A. Sarti,[19,u] C. Satriano,[26,v] A. Satta,[25] D. M. Saunders,[48] D. Savrina,[32,33] S. Schael,[9] M. Schellenberg,[10] M. Schiller,[53] H. Schindler,[40] M. Schlupp,[10] M. Schmelling,[11] T. Schmelzer,[10] B. Schmidt,[40] O. Schneider,[41] A. Schopper,[40] H. F. Schreiner,[59] K. Schubert,[10] M. Schubiger,[41] M.-H. Schune,[7] R. Schwemmer,[40] B. Sciascia,[19] A. Sciubba,[26,u] A. Semennikov,[32] A. Sergi,[47] N. Serra,[42] J. Serrano,[6] L. Sestini,[23] P. Seyfert,[21] M. Shapkin,[37] I. Shapoval,[45] Y. Shcheglov,[31] T. Shears,[54] L. Shekhtman,[36,f] V. Shevchenko,[68] B. G. Siddi,[17,40] R. Silva Coutinho,[42] L. Silva de Oliveira,[2] G. Simi,[23,q] S. Simone,[14,m] M. Sirendi,[49] N. Skidmore,[48] T. Skwarnicki,[61] E. Smith,[55] I. T. Smith,[52] J. Smith,[49] M. Smith,[55] l. Soares Lavra,[1] M. D. Sokoloff,[59] F. J. P. Soler,[53] B. Souza De Paula,[2] B. Spaan,[10] P. Spradlin,[53] S. Sridharan,[40] F. Stagni,[40] M. Stahl,[12] S. Stahl,[40] P. Stefko,[41] S. Stefkova,[55] O. Steinkamp,[42] S. Stemmle,[12] O. Stenyakin,[37] H. Stevens,[10] S. Stoica,[30] S. Stone,[61] B. Storaci,[42] S. Stracka,[24,t] M. E. Stramaglia,[41] M. Straticiuc,[30] U. Straumann,[42] L. Sun,[64] W. Sutcliffe,[55] K. Swientek,[28] V. Syropoulos,[44] M. Szczekowski,[29] T. Szumlak,[28] S. T'Jampens,[4] A. Tayduganov,[6] T. Tekampe,[10] G. Tellarini,[17,a] F. Teubert,[40] E. Thomas,[40] J. van Tilburg,[43] M. J. Tilley,[55] V. Tisserand,[4] M. Tobin,[41] S. Tolk,[49] L. Tomassetti,[17,a] D. Tonelli,[24] S. Topp-Joergensen,[57] F. Toriello,[61] R. Tourinho Jadallah Aoude,[1] E. Tournefier,[4] S. Tourneur,[41] K. Trabelsi,[41] M. Traill,[53] M. T. Tran,[41] M. Tresch,[42] A. Trisovic,[40] A. Tsaregorodtsev,[6] P. Tsopelas,[43] A. Tully,[49] N. Tuning,[43] A. Ukleja,[29] A. Ustyuzhanin,[35] U. Uwer,[12] C. Vacca,[16,l] A. Vagner,[69] V. Vagnoni,[15,40] A. Valassi,[40] S. Valat,[40] G. Valenti,[15] R. Vazquez Gomez,[19] P. Vazquez Regueiro,[39] S. Vecchi,[17] M. van Veghel,[43] J. J. Velthuis,[48] M. Veltri,[18,w] G. Veneziano,[57] A. Venkateswaran,[61] T. A. Verlage,[9] M. Vernet,[5] M. Vesterinen,[12] J. V. Viana Barbosa,[40] B. Viaud,[7] D. Vieira,[63] M. Vieites Diaz,[39] H. Viemann,[67] X. Vilasis-Cardona,[38,g] M. Vitti,[49] V. Volkov,[33] A. Vollhardt,[42] B. Voneki,[40] A. Vorobyev,[31] V. Vorobyev,[36,f] C. Voß,[9] J. A. de Vries,[43] C. Vázquez Sierra,[39] R. Waldi,[67] C. Wallace,[50] R. Wallace,[13] J. Walsh,[24] J. Wang,[61] D. R. Ward,[49] H. M. Wark,[54] N. K. Watson,[47] D. Websdale,[55] A. Weiden,[42] M. Whitehead,[40] J. Wicht,[50] G. Wilkinson,[57,40] M. Wilkinson,[61] M. Williams,[40] M. P. Williams,[47] M. Williams,[58] T. Williams,[47] F. F. Wilson,[51] J. Wimberley,[60] M. A. Winn,[7] J. Wishahi,[10] W. Wislicki,[29] M. Witek,[27] G. Wormser,[7] S. A. Wotton,[49] K. Wraight,[53] K. Wyllie,[40] Y. Xie,[65] Z. Xu,[4] Z. Yang,[3] Z. Yang,[60] Y. Yao,[61] H. Yin,[65] J. Yu,[65] X. Yuan,[61] O. Yushchenko,[37] K. A. Zarebski,[47] M. Zavertyaev,[11,b] L. Zhang,[3] Y. Zhang,[7] A. Zhelezov,[12] Y. Zheng,[63] X. Zhu,[3] V. Zhukov,[33] J. B. Zonneveld,[52] and S. Zucchelli[15]

(LHCb Collaboration)

[1]*Centro Brasileiro de Pesquisas Físicas (CBPF), Rio de Janeiro, Brazil*
[2]*Universidade Federal do Rio de Janeiro (UFRJ), Rio de Janeiro, Brazil*
[3]*Center for High Energy Physics, Tsinghua University, Beijing, China*
[4]*LAPP, Université Savoie Mont-Blanc, CNRS/IN2P3, Annecy-Le-Vieux, France*
[5]*Clermont Université, Université Blaise Pascal, CNRS/IN2P3, LPC, Clermont-Ferrand, France*

[6]CPPM, Aix-Marseille Université, CNRS/IN2P3, Marseille, France
[7]LAL, Université Paris-Sud, CNRS/IN2P3, Orsay, France
[8]LPNHE, Université Pierre et Marie Curie, Université Paris Diderot, CNRS/IN2P3, Paris, France
[9]I. Physikalisches Institut, RWTH Aachen University, Aachen, Germany
[10]Fakultät Physik, Technische Universität Dortmund, Dortmund, Germany
[11]Max-Planck-Institut für Kernphysik (MPIK), Heidelberg, Germany
[12]Physikalisches Institut, Ruprecht-Karls-Universität Heidelberg, Heidelberg, Germany
[13]School of Physics, University College Dublin, Dublin, Ireland
[14]Sezione INFN di Bari, Bari, Italy
[15]Sezione INFN di Bologna, Bologna, Italy
[16]Sezione INFN di Cagliari, Cagliari, Italy
[17]Universita e INFN, Ferrara, Ferrara, Italy
[18]Sezione INFN di Firenze, Firenze, Italy
[19]Laboratori Nazionali dell'INFN di Frascati, Frascati, Italy
[20]Sezione INFN di Genova, Genova, Italy
[21]Universita & INFN, Milano-Bicocca, Milano, Italy
[22]Sezione di Milano, Milano, Italy
[23]Sezione INFN di Padova, Padova, Italy
[24]Sezione INFN di Pisa, Pisa, Italy
[25]Sezione INFN di Roma Tor Vergata, Roma, Italy
[26]Sezione INFN di Roma La Sapienza, Roma, Italy
[27]Henryk Niewodniczanski Institute of Nuclear Physics Polish Academy of Sciences, Kraków, Poland
[28]AGH - University of Science and Technology, Faculty of Physics and Applied Computer Science, Kraków, Poland
[29]National Center for Nuclear Research (NCBJ), Warsaw, Poland
[30]Horia Hulubei National Institute of Physics and Nuclear Engineering, Bucharest-Magurele, Romania
[31]Petersburg Nuclear Physics Institute (PNPI), Gatchina, Russia
[32]Institute of Theoretical and Experimental Physics (ITEP), Moscow, Russia
[33]Institute of Nuclear Physics, Moscow State University (SINP MSU), Moscow, Russia
[34]Institute for Nuclear Research of the Russian Academy of Sciences (INR RAN), Moscow, Russia
[35]Yandex School of Data Analysis, Moscow, Russia
[36]Budker Institute of Nuclear Physics (SB RAS), Novosibirsk, Russia
[37]Institute for High Energy Physics (IHEP), Protvino, Russia
[38]ICCUB, Universitat de Barcelona, Barcelona, Spain
[39]Universidad de Santiago de Compostela, Santiago de Compostela, Spain
[40]European Organization for Nuclear Research (CERN), Geneva, Switzerland
[41]Institute of Physics, Ecole Polytechnique Fédérale de Lausanne (EPFL), Lausanne, Switzerland
[42]Physik-Institut, Universität Zürich, Zürich, Switzerland
[43]Nikhef National Institute for Subatomic Physics, Amsterdam, Netherlands
[44]Nikhef National Institute for Subatomic Physics and VU University Amsterdam, Amsterdam, Netherlands
[45]NSC Kharkiv Institute of Physics and Technology (NSC KIPT), Kharkiv, Ukraine
[46]Institute for Nuclear Research of the National Academy of Sciences (KINR), Kyiv, Ukraine
[47]University of Birmingham, Birmingham, United Kingdom
[48]H.H. Wills Physics Laboratory, University of Bristol, Bristol, United Kingdom
[49]Cavendish Laboratory, University of Cambridge, Cambridge, United Kingdom
[50]Department of Physics, University of Warwick, Coventry, United Kingdom
[51]STFC Rutherford Appleton Laboratory, Didcot, United Kingdom
[52]School of Physics and Astronomy, University of Edinburgh, Edinburgh, United Kingdom
[53]School of Physics and Astronomy, University of Glasgow, Glasgow, United Kingdom
[54]Oliver Lodge Laboratory, University of Liverpool, Liverpool, United Kingdom
[55]Imperial College London, London, United Kingdom
[56]School of Physics and Astronomy, University of Manchester, Manchester, United Kingdom
[57]Department of Physics, University of Oxford, Oxford, United Kingdom
[58]Massachusetts Institute of Technology, Cambridge, Massachusetts, USA
[59]University of Cincinnati, Cincinnati, Ohio, USA
[60]University of Maryland, College Park, Maryland, USA
[61]Syracuse University, Syracuse, New York, USA
[62]Pontifícia Universidade Católica do Rio de Janeiro (PUC-Rio), Rio de Janeiro, Brazil
(associated with Institution Universidade Federal do Rio de Janeiro (UFRJ), Rio de Janeiro, Brazil)
[63]University of Chinese Academy of Sciences, Beijing, China
(associated with Institution Center for High Energy Physics, Tsinghua University, Beijing, China)

[64]*School of Physics and Technology, Wuhan University, Wuhan, China*
(associated with Institution Center for High Energy Physics, Tsinghua University, Beijing, China)
[65]*Institute of Particle Physics, Central China Normal University, Wuhan, Hubei, China*
(associated with Institution Center for High Energy Physics, Tsinghua University, Beijing, China)
[66]*Departamento de Fisica, Universidad Nacional de Colombia, Bogota, Colombia*
(associated with Institution LPNHE, Université Pierre et Marie Curie, Université Paris Diderot, CNRS/IN2P3, Paris, France)
[67]*Institut für Physik, Universität Rostock, Rostock, Germany*
(associated with Institution Physikalisches Institut, Ruprecht-Karls-Universität Heidelberg, Heidelberg, Germany)
[68]*National Research Centre Kurchatov Institute, Moscow, Russia*
(associated with Institution Institute of Theoretical and Experimental Physics (ITEP), Moscow, Russia)
[69]*National Research Tomsk Polytechnic University, Tomsk, Russia*
(associated with Institution Institute of Theoretical and Experimental Physics (ITEP), Moscow, Russia)
[70]*Instituto de Fisica Corpuscular, Centro Mixto Universidad de Valencia - CSIC, Valencia, Spain*
(associated with Institution ICCUB, Universitat de Barcelona, Barcelona, Spain)
[71]*Van Swinderen Institute, University of Groningen, Groningen, Netherlands*
(associated with Institution Nikhef National Institute for Subatomic Physics, Amsterdam, Netherlands)

[a]Also at Università di Ferrara, Ferrara, Italy.
[b]Also at P.N. Lebedev Physical Institute, Russian Academy of Science (LPI RAS), Moscow, Russia.
[c]Also at AGH - University of Science and Technology, Faculty of Computer Science, Electronics and Telecommunications, Kraków, Poland.
[d]Also at Università di Milano Bicocca, Milano, Italy.
[e]Also at Università di Modena e Reggio Emilia, Modena, Italy.
[f]Also at Novosibirsk State University, Novosibirsk, Russia.
[g]Also at LIFAELS, La Salle, Universitat Ramon Llull, Barcelona, Spain.
[h]Also at Università di Bologna, Bologna, Italy.
[i]Also at Università di Roma Tor Vergata, Roma, Italy.
[j]Also at Università di Genova, Genova, Italy.
[k]Also at Scuola Normale Superiore, Pisa, Italy.
[l]Also at Università di Cagliari, Cagliari, Italy.
[m]Also at Università di Bari, Bari, Italy.
[n]Also at Laboratoire Leprince-Ringuet, Palaiseau, France.
[o]Also at Università degli Studi di Milano, Milano, Italy.
[p]Also at Universidade Federal do Triângulo Mineiro (UFTM), Uberaba-MG, Brazil.
[q]Also at Università di Padova, Padova, Italy.
[r]Also at Iligan Institute of Technology (IIT), Iligan, Philippines.
[s]Also at Hanoi University of Science, Hanoi, Vietnam.
[t]Also at Università di Pisa, Pisa, Italy
[u]Also at Università di Roma La Sapienza, Roma, Italy.
[v]Also at Università della Basilicata, Potenza, Italy.
[w]Also at Università di Urbino, Urbino, Italy.